Gravity: Jurnal Ilmiah Penelitian dan Pembelajaran Fisika
http://jurnal.untirta.ac.id/index.php/Gravity
ISSN: 244-515x; e-ISSN: 2528-1976
Vol. 10, No. 2, August 2024, Page 101-116

Investigation of the potential use of Water-CuO nanofluids for energy extraction in abandoned geothermal wells

Syaharussajali*, Suyanto, Ruri Agung Wahyuono

Department of Engineering Physics, Institute Teknologi Sepuluh November, Indonesia

**E-mail: Syaharussajali74@gmail.com*

(Received: 28 July 2024; Accepted: 22 August 2024; Published: 30 August 2024)

ABSTRACT

Indonesia has a geothermal potential of 24 Gigawatts (GW), making Indonesia the second largest country with geothermal potential. High investment costs are still a challenge in the development of geothermal energy, where the cost of drilling geothermal wells is the most expensive with a cost of more than 50% of the total project cost. One solution to this problem is retrofitting abandoned wells with a closed loop well system (double pipe heat exchanger). Reusing abandoned wells to extract heat energy only costs about a third of the cost of making a new geothermal well. However, the low heat transfer value of this system makes it rarely applied as a power plant. Therefore, the thesis research analyzes the effect of adding CuO nanoparticles in the base fluid (water) of a double pipe well as a solution to improve heat transfer performance. The effect of nanoparticles on closed loop wells is modeled using a CFD simulation approach. The results of the CFD simulation will be used as input in calculating the performance of the Organic Rankine Cycle system which is used to determine the potential for electricity generation. Based on the calculation results, it was obtained that CuO nanoparticles with a concentration of 4%wt had the greatest heat transfer among other nanoparticle variations and this was in line with the power output produced, which was 2045 kW.

Keywords : CFD, ORC, Retrofitting abandoned wells.

DOI: 10.30870/gravity.v10i2.27892

INTRODUCTION

Indonesia has a geothermal potential of 24 Gigawatts (GW), making Indonesia the second largest country with geothermal potential. High investment costs are still a challenge in the development of geothermal energy, where the cost of drilling geothermal wells is the most expensive with a cost of more than 50% of the total project cost. One solution to this problem is retrofitting abandoned wells with a closed loop well system (double pipe heat exchanger). Reusing abandoned wells to extract heat energy only costs about one third of making a new

geothermal well. However, the low heat transfer value of this system makes it rarely applied as a power plant. Therefore, this study analyzes the effect of adding CuO core-shell nanoparticles in water-based fluids in double pipe wells as a solution to improve the performance of thermal energy extraction used for heating the evaporator in the Organic Rankine Cycle.

CuO nanoparticles were synthesized using a wet chemistry approach where the nanocomposite structure was intended to obtain a high thermal conductivity contribution from CuO nanoparticles. CuO nanofluids were characterized by several properties such as thermal conductivity and viscosity. The effect of CuO nanofluid composition on heat extraction in a closed loop well will be modeled using a Computational Fluid Dynamics (CFD) simulation approach. The CFD simulation results were used as input in calculating the performance of the Organic Rankine Cycle system to determine the potential for electricity generation with Unisim software. And to the best of our knowledge writer that Not yet There is study related nanoparticles *CuO* For utilized as suspended material in fluids water work for increase performance extraction energy in *abandoned wells.*

RESEARCH METHODS

1. Well Properties Data Collection

System *closed loop well* working principle by circulating fluid into the *well* that's the configuration in cycle closed. System *closed loop well* divided into two types , double pipe/co-axial and U-tube heat exchanger. Based on its application for extraction energy from *abandoned well*, double pipe commonly used because of its has wide surface that can increase *heat* transfer height which will increase thermal efficiency of *closed loop well* , low pressure drop , and minimizes use of grout (Alimonti et al., 2019; Cheng et al., 2019; Kurnia et al., 2021; Schiffner et al., 2022; Wang et al., 2018) . Appearance illustration of double pipe and U-tube can seen in figure 1.

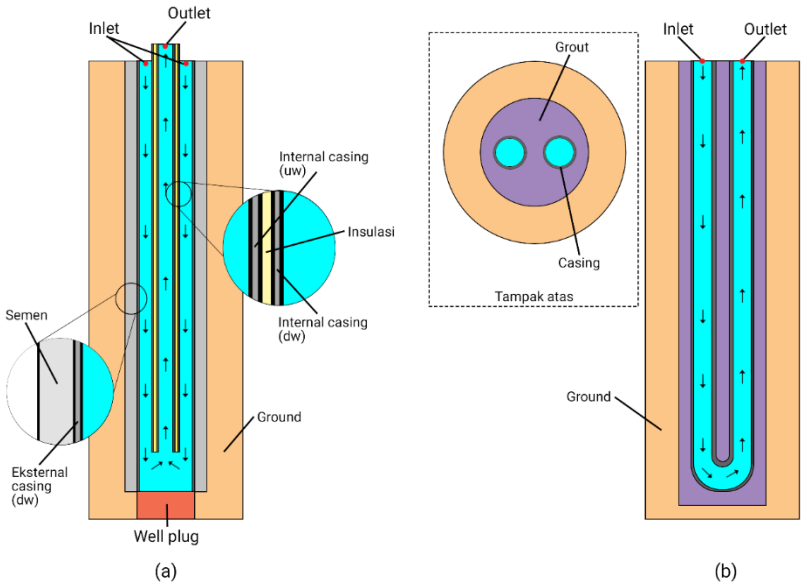

Figure 1. Appearance form *well* double pipe (a) and U-tube (b

Heat transfer is one of the important aspects in a closed loop well system, in analyzing the heat transfer that occurs between the fluid and the wellbore, thermal resistance can be used. This analysis refers to the analysis conducted by Alimonti C et al. Thermal resistance is divided into two main parts, namely heat transfer between the fluid that goes into the wellbore with rocks and heat transfer between the fluid that goes out of the wellbore with the insulation wall and steel casing. (Alimonti et al., 2019) .

Thermal resistance (R_s) between surface external *well* casing and rocks around *wellbore* can estimated with line heat source theory with assumption wall *well* nature conductive and slender geometry (thin and long). R_s can stated in equation (2.1) (Alimonti et al., 2019) .

$$R_s = \frac{1}{2\pi\lambda_s}\ln\left(\frac{2\sqrt{\alpha_s t}}{r_{o,1}}\right) \tag{1}$$

Where λ_s is the thermal conductivity of the soil (W/ mK), α_s is the thermal diffusivity of the soil (m^2/s), and $r_{o,1}$ is the outer radius of the external casing . Meanwhile, for the thermal resistance between the fluid and the external and internal casing well, the classical Dittus Boelter equation is used to calculate the convection coefficient. R_a defines the equation for the thermal resistance of the fluid that goes to the wellbore with the external casing well and R_b defines the equation for the thermal resistance of the fluid that exits the wellbore with the internal casing well. Ra and Rb are formulated in equations (2) and (3) below. (Alimonti et al., 2019)

$$R_a = R_s + \frac{\ln\left(\frac{r_{o,1}}{r_{i,1}}\right)}{2\pi\lambda_1} + \frac{1}{2\pi r_{o,2}k_{w,downward}} \tag{2}$$

$$R_b = \frac{1}{2\pi r_{i,2}k_{w,downward}} + \sum_{j=3}^{5}\frac{\ln\left(\frac{r_{o,j}}{r_{i,j}}\right)}{2\pi\lambda_j} + \frac{1}{2\pi r_{i,5}k_{w,upward}} \tag{3}$$

Where k_w is the conductivity of water (W/mK), λ_1 is the external thermal conductivity of the casing, λ_3 is the internal thermal conductivity of the casing (dw) and $r_{o,1}$, $r_{i,1}$, $r_{o,2}$, $r_{i,2}$, $r_{o,3}$, $r_{i,3}$ $r_{i,5}$ in sequence are the radii (m) of the outer external casing, inner external casing, outer water *downward* , inner water *downward* , outer internal casing (dw), inner internal casing (dw), and inner internal casing (uw). then for total *heat transfer* can use equation (4) below.

$$\dot{Q} = \dot{m}_w c_w (T_{1,w} - T_{5,w}) \tag{4}$$

Where $\dot{Q}$ is the thermal power (W), $\dot{m}_w$is the water flow rate (kg/s), $c_w$is *the specific heat capacity* of water (J/ kg.K), T $_{1,w}$ profile temperature external casing and T $_{5,w}$ is profile temperature fluid throughout *wellbore closed loop well* estimated with equation (5) below.

$$\dot{m}_w c_w \frac{dT_{w,downward}}{dz}(z) = \frac{T_s(z) - T_{w,downward}(z)}{R_a} - \frac{T_{w,downward}(z) - T_{w,upward}(z)}{R_b} \quad (5)$$

$$-\dot{m}_w c_w \frac{dT_{w,upward}}{dz}(z) = \frac{T_{w,downward}(z) - T_{w,upward}(z)}{R_b}$$

With boundary conditions as following :

$$T_{w,downward}(0) = T_{1,w} \quad (6)$$

$$T_{w,downward}(L) = T_{w,upward}(L)$$

This equation (5) Then will completed in a way numeric with CFD approach to get the outlet temperature T $_{5,w}$ = T $_{w,upward}$ (0) as function rate flow mass and inlet temperature T $_{1,w}$.

Well data and well wall material properties were obtained from a well abandoned by a geothermal company. The company chose not to publish its identity and the origin of this well to maintain confidentiality. Therefore, this well will be given the initials well-TMB. Some parameters obtained from the geothermal company include well depth, surface temperature, and well temperature distribution which is generally linearly distributed with well depth. Meanwhile, the well wall material properties were obtained from the research of Chapidi et al. The following is the geometric dimension data of the well provided by the company.

Table 1. Well-TMB geometric parameter

Parameter	Unit	Value
Well depth	m	280
Land diameter from bore	m	40
Bore diameter	m	0.35
Outer diameter external casing	m	0.35
External casing thickness	m	0.02
Outer internal diameter of casing (dw)	m	0.2
internal casing (dw) thickness	m	0.01
Insulation thickness	m	0.01
Outer internal diameter of casing (uw)	m	0.16
internal casing (uw) thickness	m	0.01

Based on research conducted by chapidi et al, the soil structure at a depth of less than 1000 meters is generally still dominated by sandstone. In addition, casing and insulation materials

are also quoted from the research of chapidi et al. The following are the properties of sandstone, casing, and insulation used in the simulation.

Table 2. Properties of well-TMB structure material (Chappidi et al., 2023)

Material properties	Specific heat capacity (J/ kg.K)	Thermal cond (W/ mK)	Density (kg/m3)
Insulation properties	1100	0.02	1400
Casing	502.48	16.27	8030
Sandstone	873.62	2.64	2300

From the company, temperature distribution data against well depth was also obtained. The data was then plotted and regressed to obtain a function equation that would later be used in CFD simulation as a user defined function (UDF). It can be seen in Figure 2 that the temperature distribution against well depth tends to be linear with a square root of 0.98.

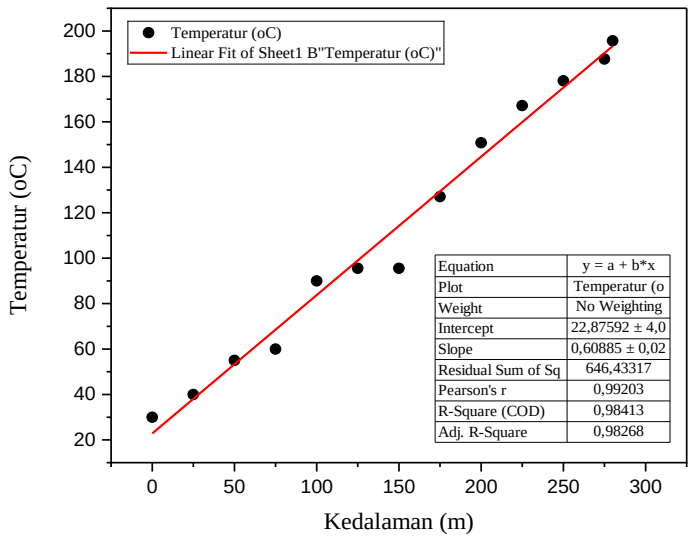

Figure 2. Regression results of temperature data against well depth·

2. Properties of Nanoparticles

Nanoparticles can be applied in various fields, one of which is as an additional material to improve heat transfer performance. Nanoparticles improve heat transfer performance by increasing the thermal conductivity value. There are various variables that affect the thermal conductivity value of nanoparticles, including the size of the particle diameter. (Farajollahi et al., 2010; Maheshwary et al., 2017; Younes et al., 2022) , fluid pH (Leong et al., 2018; Sajid & Ali, 2018; Xie et al., 2002) , and the type nanoparticles used (Abdollahi & Shams, 2015; Ajeeb et al., 2023; Du et al., 2020; Farajollahi et al., 2010; Garoosi et al., 2016; Hemmat Esfe, 2017; Maheshwary et al., 2017; Mohammed et al., 2018; Qu et al., 2023; Safaei et al., 2020; Shingare et al., 2012; Younes et al., 2022) .

The addition of nanoparticles to the base fluid can change several thermal properties of the fluid such as density, specific heat capacity, thermal conductivity, and viscosity. The addition of nanoparticles in small concentrations to the base fluid can increase the density of the mixture, the density of the nanofluid can be calculated using the following equation (7). (Salameh et al., 2023) .

$$\rho_{nf} = \varphi\rho_p + (1-\varphi)\rho_{bf} \tag{7}$$

Where ρ_{nf} is the density of the nanofluid (kg/m ^{3}), ρ_p is the density of the nanoparticles (kg/m ^{3}), ρ_{bf} is the density of *the base fluid* (kg/m ^{3}), and φ is the concentration of nanoparticles added into *the base fluid* (% wt). Meanwhile, the specific heat capacity of nanofluids is a mixture of the specific heat capacity of nanoparticles and base fluids according to the energy balance formulated in the following equation. (Chappidi et al., 2023)

$$C_{pnf} = \frac{(1-\varphi)\rho_{bf}C_{pbf} + \varphi\rho_{np}C_{pnp}}{\rho_{nf}} \tag{8}$$

Where C_{pnf}, C_{pbf}, C_{pnp} are respectively *the specific heat capacity* (J/ kg.K) of nanofluids , *base fluids* , and nanoparticles . The formulation related to the thermal conductivity of nanofluids generally uses the Maxwell theory model which is based on the classical effective medium theory (EMT), however the theory with the EMT model assumes that the particles are distributed evenly and statically without considering the movement of particles (Brownian motion) in the base fluid (Coccia et al., 2021) . Research conducted by Jang and Choi formulated a thermal conductivity equation that considers various modes of energy transport in nanofluids such as collisions between base fluid molecules, thermal diffusion of nanoparticles, and collisions between nanoparticles through translational motion due to Brownian motion. The following is the thermal conductivity equation in nanofluids.

$$\frac{k_{nf}}{k_{bf}} = 1 + 4,4\,\mathrm{Re}^{0,4}\,\mathrm{Pr}^{0,66}\left(\frac{T}{T_{fr}}\right)^{10}\left(\frac{k_{np}}{k_{bf}}\right)^{0,03}\varphi^{0,66} \tag{9}$$

Where k_{nf}, k_{bf}, k_{np} are thermal conductivity (W/m K) of nanofluids , *base fluids* , and nanoparticles respectively. T_{fr} is point freezing temperature of base fluid, *Pr* is the Prandtl number of the base fluid, and *Re* is the Reynolds number defined with equality following

$$\mathrm{Re} = \frac{2\rho_{bf}k_B T}{\pi\mu_{bf}^2 d_{np}} \tag{10}$$

Where is T is the fluid temperature , k_B Boltzmann's constant , d_p is the diameter of the nanoparticle (Jang & Choi, 2004) .

Brinkman proposed a model for determine viscosity from fluid containing nanoparticles . This model is also valid for concentration low nanoparticles (0-4 % wt) (Klazly & Bognár, 2022) . Viscosity nanofluids defined in equation (11).

$$\mu_{nf} = \frac{1}{(1-\varphi)^{2,5}} \mu_{bf} \tag{11}$$

Where μ_{nf} and μ_{bf} are the viscosities of the nanofluid and *base fluid* .
Characteristics nanoparticles CuO used in this study obtained from research data Vajjha et al. Following table are physical property from nanoparticles CuO .

Table 3. Properties of CuO nanoparticles

Nanoparticles	Density (kg/ ^{m3})	Specific heat (J/kg.K)	Thermal conductivity (W/mK)	Particle diameter (nm)
CuO	6500	525	17.65	29

The addition of nanoparticles to the base fluid affects the characteristics of thermal nanofluids. Changes in these thermal characteristics will later affect heat transfer which results in an increase in the outlet temperature of the double pipe well. The values of these thermal characteristics are obtained from the calculation results with equations (7) to (11). The following are the thermal properties of nanofluids with variations in material type and concentration.

Table 4. Thermal characteristics of nanofluids

Concentration (% wt)	Density (kg/m3)	Specific heat capacity (J/kg K)	Thermal conductivity (W/ mK)
0.20%	998.03	4134.36	0.920
0.50%	1014.57	4064.85	1,149
1.00%	1042.13	3953.90	1,442
2.00%	1097.26	3748.73	1,905
4.00%	1207.52	3394.58	2,637

3. CFD Numerical Simulation

Computational fluid dynamics (CFD) is one of the numerical approaches to solve physical phenomena such as air flow, heat distribution and so on. In CFD simulation consists of three main stages, namely determining the geometry model, meshing, and setup. In this study, the geometry structure of the wellbore which is changed into a double pipe will be modeled in a 2D-axisymmetric model. This model provides fairly accurate heat transfer prediction results between the well and the surrounding rocks with a relatively faster computing time. (Chappidi et al., 2023; Cheng et al., 2019).

Another assumption used in this study is the constant inlet fluid and well temperatures, to model different temperature distributions as the well depth increases, using a user defined function (UDF) written in the C programming language. The data in this UDF modeling was

obtained from the Geothermal Company as the study case location. In CFD simulation, Semi-Implicit Pressure Linked Equation (SIMPLE) is an algorithm used to connect pressure and velocity with second order discretization in solving computational problems because of its reliability (Chappidi et al., 2023; Cheng et al., 2019; Jery et al., 2023).

In CFD simulation, the initial stage is to prepare geometry that can represent the existing condition, this simulation uses 2D geometry because the well geometry is symmetrical. Then the geometry will be discretized into finite elements (mesh) so that the computation process can be carried out. The following is a display of geometry and mesh in this research simulation.

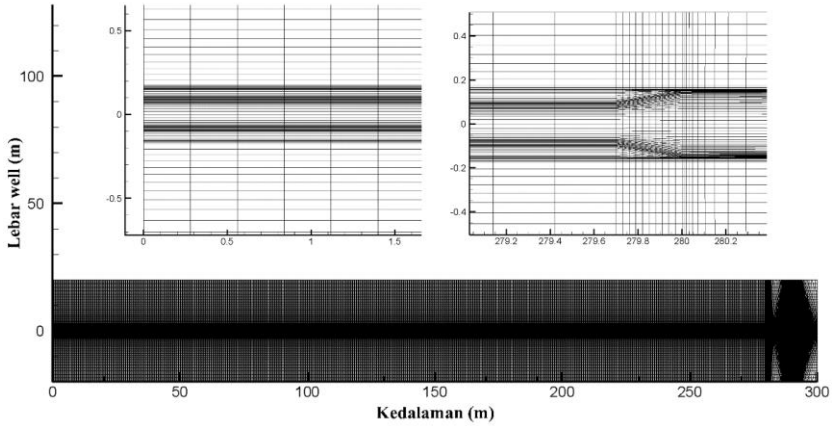

Figure 3. 2D view of geometry and mesh

The size and shape of the mesh used in the simulation greatly affect the simulation results. These results will not change after a certain domain refinement stage and at that point, the numerical domain that has gone through the refinement stage is known as the independent mesh and its stages are known as mesh sensitivity analysis. In this sensitivity analysis, the output parameters of the outlet well temperature and skewness will be used. The following is a table of mesh sensitivity analysis results..

Table 5. Independent mesh results

No	Number of elements	Number of nodes	Skewness	temperature (K)	Error
1	192528	193843	0.15	409.60	
2	172200	173394	0.28	409.63	0.0073%
3	144648	145678	0.33	409.62	0.0049%
5	61320	61854	0.58	409.60	0.0000%

Based on table 5, it can be seen that the error in the variation of the number of elements from 1 to 5 is relatively very small, but in the first variation the skewness value is very low when compared to other variations. Therefore, this research simulation will use mesh variation 1.

4. Organic Rankine Cycle (ORC) Simulation

In this ORC process scheme, a double parallel well will be used to achieve the target of 1 MW of electrical energy. The ORC process diagram that will be used in this study is shown in Figure 4.

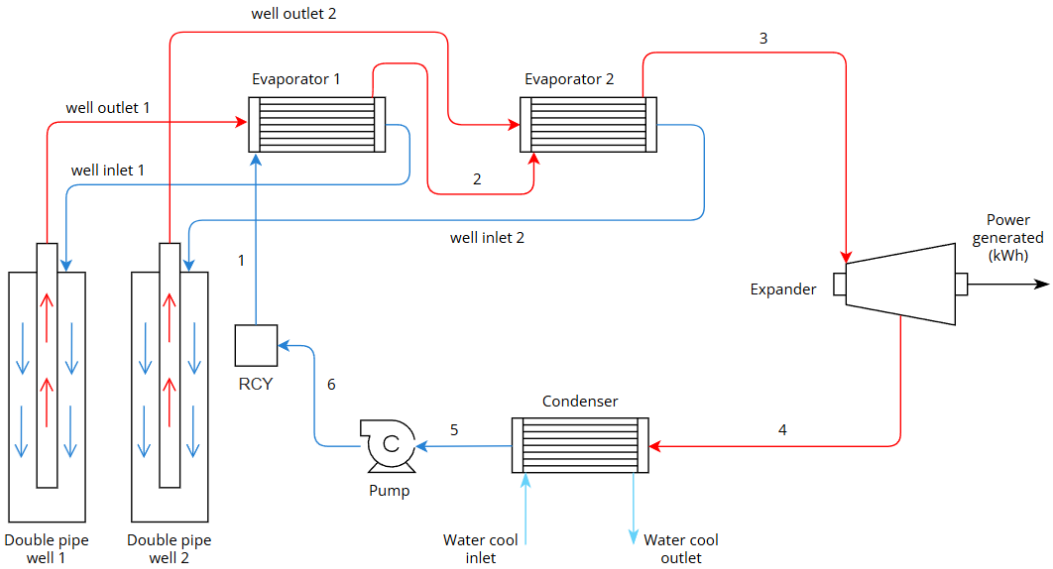

Figure 4. Schematic of organic rankine cycle process with double well.

In determining the working fluid used in the ORC system, it is necessary to consider several criteria such as low critical pressure and temperature (compared to water), specific volume, high thermal conductivity, non-corrosive, toxic/flammable and stable. Meanwhile, based on the working fluid that is often used in the ORC cycle, isopentane is the most commonly used because it can increase the specific net power output by up to 40% (Vetter et al., 2013) . ORC simulation will use Unisim software. Temperature, flow, and outlet well pressure data from the CFD simulation results will be used as input for the energy and exergy simulation of the ORC system. The simulation process begins by defining the working fluid to be used and inputting the thermodynamic model, in this simulation the thermodynamic model used is Peng-Robinson which is suitable for hydrocarbon working fluids such as isopentane.

This simulation is highly dependent on the flow rate of the working fluid circulating in the double pipe well. The flow rate in the double pipe well used in this study to obtain a minimum power output of 1 MW is 30 kg / s with temperature and pressure depending on the results of the CFD simulation. The flow rate in the isopentane working fluid is 15 kg / s and the flow rate in the cooling water is 30 kg / s. In addition, the pressure drop in the evaporator and condenser is set at around 0.2 bar. This value is generally used in designing heat exchangers.

RESULTS AND DISCUSSION

1. Characteristics of nanofluids

Based on Figure 5, it can be seen that the thermal properties of nanofluids increase with increasing concentration of CuO nanoparticles. CuO shows the highest thermal conductivity at

a concentration of 4%. The high thermal conductivity of CuO nanofluids can be explained by the intrinsic properties of CuO nanoparticles themselves which have excellent thermal conductivity. Previous studies have confirmed that CuO is often used in thermal conductivity enhancement applications due to its high thermal conductivity value compared to many other nanoparticles.

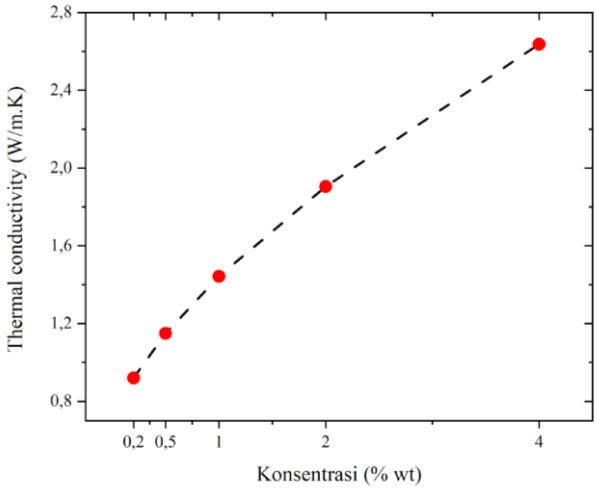

Figure 5. Thermal conductivity (W/mK) of CuO against concentration (% wt)

2. Effect of Addition of Nanofluids

The thermal performance of the double pipe well with nanofluid working fluid is shown in Figure 6 which is obtained based on the outlet temperature of the double pipe well. The simulation was carried out by varying the concentration of nanoparticles from 0.2% to 4%. From Figure 6, it can be seen that the outlet temperature increases linearly with increasing nanoparticle concentration. The maximum increase in the outlet temperature of the double pipe well occurs when the CuO concentration is 4% wt which can increase the temperature by 16.5 ^{o}C or an increase of 12.8% when compared to using water. While the lowest increase occurs at a concentration of 0.2%. The significant increase in outlet temperature at high concentrations of CuO is generally due to the greater thermal conductivity of CuO, so as the concentration increases, more particles can transfer heat.

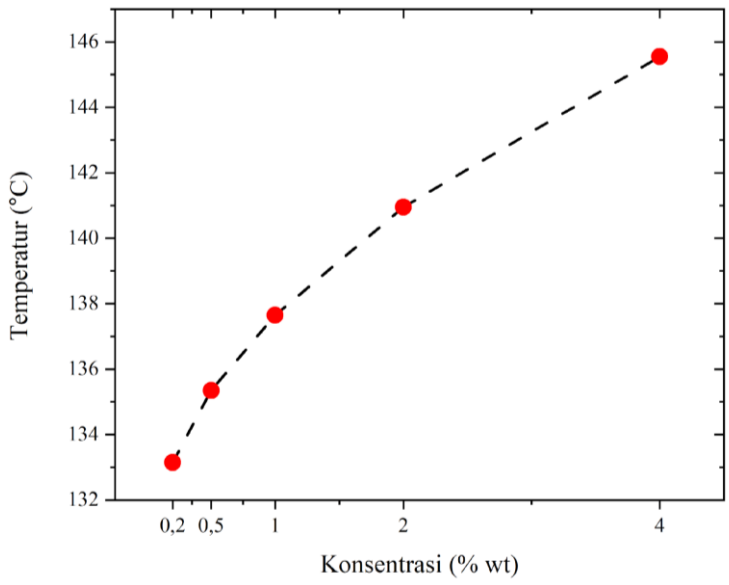

Figure 6. Graph of outlet temperature against nanoparticle concentration

Figure 7 shows the results of the temperature contour simulation against well depth. The temperature distribution against well depth refers to a linear regression equation where the temperature tends to increase linearly with increasing depth. Based on the temperature distribution, the results of the simulation distribution compared to the existing data are in accordance with the existing well temperature where the temperature on the ground surface is around 30 ºC and the temperature at a depth of 300 m is around 180 ºC.

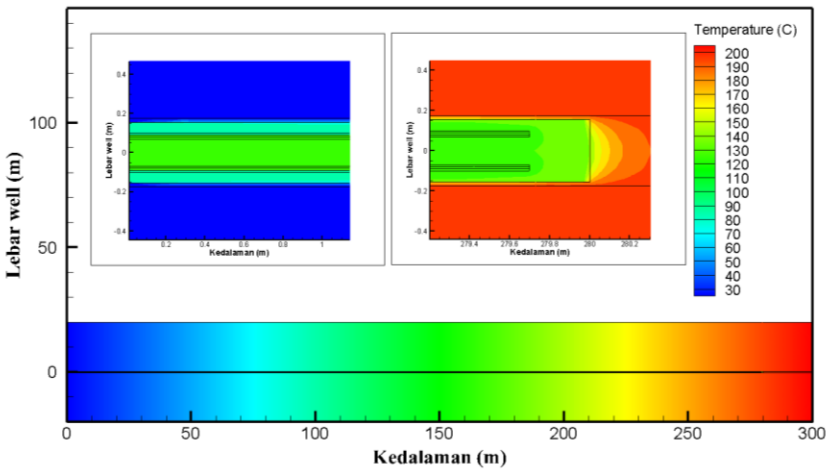

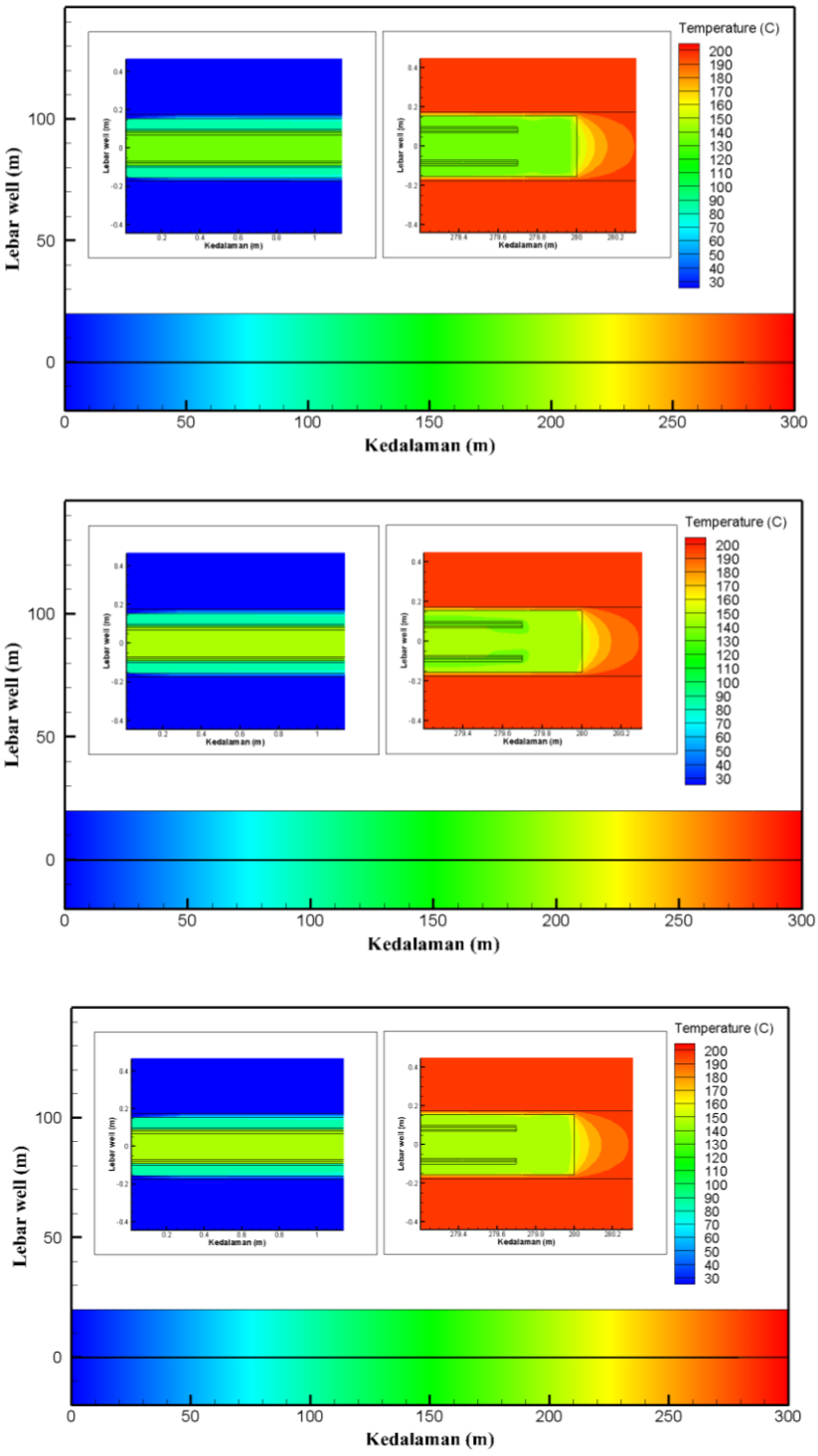

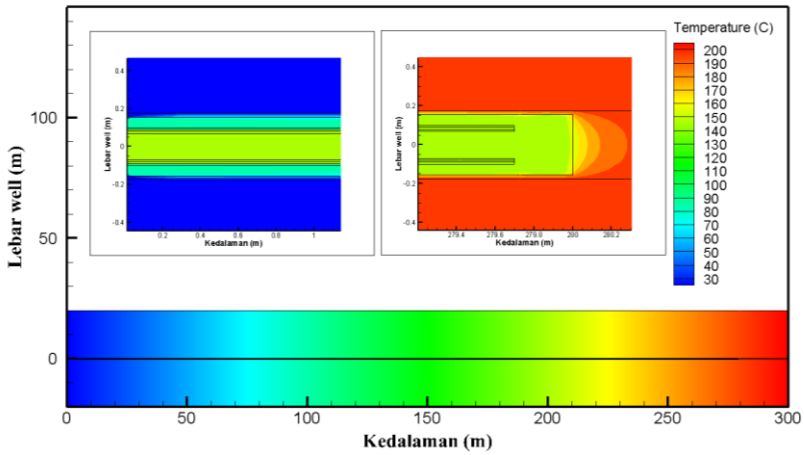

Figure 7. Appearance CFD simulation temperature distribution of double pipe well fluid Work nanofluids CuO concentrations of 0.2%, 0.5%, 1%, 2%, and 4%wt in order from on to lower .

3. Analysis Exergy

Figures 8 and 9 show the power output and the percent increase in power output from the ORC cycle after the addition of nanoparticles to the working fluid of the double pipe well. It can be seen that the power output tends to increase as the concentration of nanoparticles increases. The highest increase occurs in CuO with a concentration of 4% producing a power output of 2045 kW or about 78% increase when compared to water which only produces a power output of 1142 kW. This increase in power output is caused by an increase in the outlet temperature of the well as the concentration increases which causes heat transfer to the ORC cycle to increase.

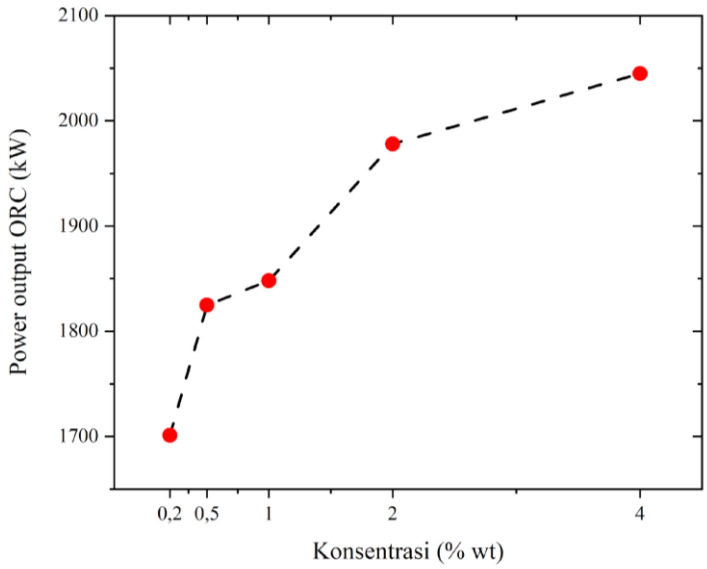

Figure 8 . ORC power output graph (kW) against nanoparticle concentration

Based on Figure 9, it can be seen that there is an increase in power from 47% to 78% when compared to the double pipe well which only uses water as the working fluid. The most

significant increase in ORC power output ratio occurs in the CuO nanoparticle type, this is due to the higher thermal conductivity of CuO when compared to ZnO@TiO2 and TiO2 core-shell nanoparticles.

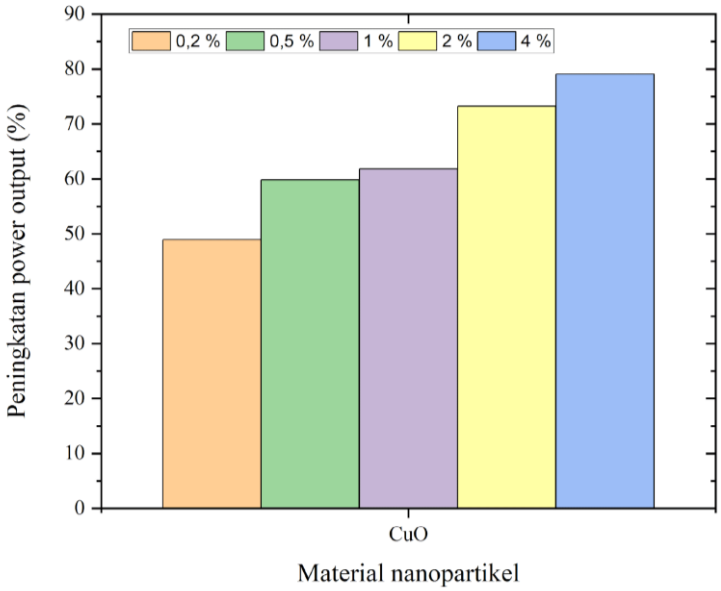

Figure 9. The results of increasing power output against variations in the type and concentration of nanoparticles.

Figure 10 shows the percentage of exergy destruction of each equipment in the ORC generation cycle. The highest exergy destruction occurs in the condenser during the heat exchange process, followed by the expander, evaporator 2, evaporator 1, and pump. Overall, the total exergy destruction in this ORC cycle is 2033 kW. This exergy destruction mapping is important to see the potential for improvements that need to be made to increase the efficiency of the ORC double pipe well.

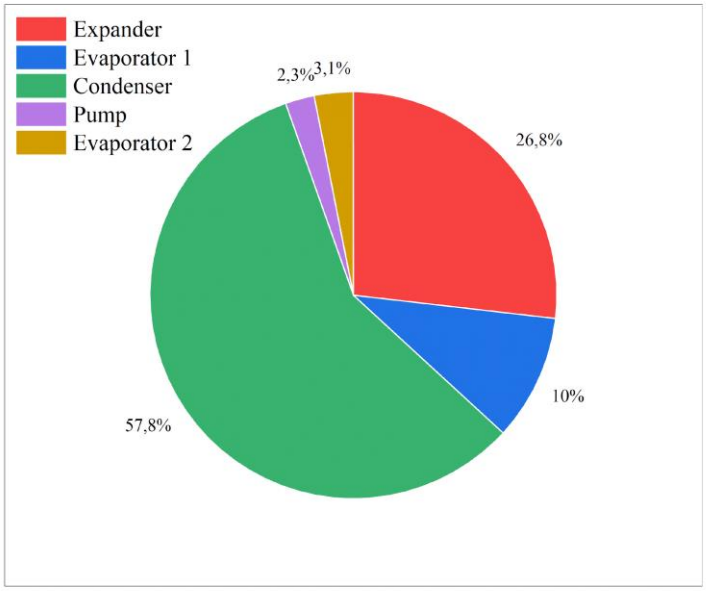

Figure 10. The results of the distribution of exergy destruction in each equipment in the ORC

CONCLUSION

The addition of CuO nanoparticles in the base fluid (water) can increase the outlet temperature of the double pipe well and increase the power output of the ORC cycle. The maximum increase in the outlet temperature of the double pipe well occurs when the CuO concentration is 4% wt which can increase the temperature by 16.5 ºC or an increase of 12.8%. Then the highest increase in power output occurs in CuO with a concentration of 4% producing a power output of 2045 kW or an increase of about 78% when compared to water which only produces a power output of 1142 kW. This increase in power output is caused by an increase in the outlet temperature of the well as the concentration increases which causes heat transfer to the ORC cycle to increase

REFERENCES

Abdollahi, A., & Shams, M. (2015). Optimization of heat transfer enhancement of nanofluid in a channel with winglet vortex generator. *Applied Thermal Engineering , 91* , 1116–1126. https://doi.org/10.1016/j.applthermaleng.2015.08.066

Ajeeb, W., Thieleke da Silva, R.R.S., & Murshed, SMS (2023). Experimental investigation of heat transfer performance of Al2O3 nanofluids in a compact plate heat exchanger. *Applied Thermal Engineering , 218* (September 2022). https://doi.org/10.1016/j.applthermaleng.2022.119321

Alimonti, P, C., & E, S. (2019). A comprehensive exergy evaluation of a deep borehole heat exchanger coupled with an ORC plant: the case study of Campi Flegrei. *Energy , 189* . https://doi.org/10.1016/j.energy.2019.116100

Chappidi, S., Kumar, A., & Singh, J. (2023). Geothermal energy extraction from abandoned oil and gas wells using mono and hybrid nanofluids. *Geothermics , 114* (May). https://doi.org/10.1016/j.geothermics.2023.102794

Cheng, SWY, Kurnia, JC, Ghoreishi-Madiseh, SA, & Sasmito, AP (2019). Optimization of geothermal energy extraction from abandoned oil well with a novel well bottom curvature design using Taguchi method. *Energy , 188* . https://doi.org/10.1016/j.energy.2019.116098

Coccia, G., Tomassetti, S., & Di Nicola, G. (2021). Thermal conductivity of nanofluids: A review of the existing correlations and a scaled semi-empirical equation. *Renewable and Sustainable Energy Reviews , 151* (January). https://doi.org/10.1016/j.rser.2021.111573

Du, R., Jiang, D.D., Wang, Y., & Wei Shah, K. (2020). An experimental investigation of CuO/water nanofluid heat transfer in geothermal heat exchanger. *Energy and Buildings* , *227* . https://doi.org/10.1016/j.enbuild.2020.110402

Farajollahi, B., Etemad, S. G., & Hojjat, M. (2010). Heat transfer of nanofluids in a shell and tube heat exchanger. *International Journal of Heat and Mass Transfer , 53* (1–3), 12–17. https://doi.org/10.1016/j.ijheatmasstransfer.2009.10.019

Garoosi, F., Hoseininejad, F., & Rashidi, M. M. (2016). Numerical study of heat transfer performance of nanofluids in a heat exchanger. *Applied Thermal Engineering , 105* , 436–455. https://doi.org/10.1016/j.applthermaleng.2016.03.015

Hemmat Esfe, M. (2017). Designing a neural network for predicting the heat transfer and pressure drop characteristics of Ag/water nanofluids in a heat exchanger. *Applied Thermal Engineering , 126* , 559–565. https://doi.org/10.1016/j.applthermaleng.2017.06.046

Jang, S.P., & Choi, S.U.S. (2004). Role of Brownian motion in the enhanced thermal

conductivity of nanofluids. *Applied Physics Letters* , *84* (21), 4316–4318. https://doi.org/10.1063/1.1756684

Jery, A. El, Khudhair, AK, Abbas, SQ, Abed, AM, & Khedher, KM (2023). Numerical simulation and artificial neural network prediction of hydrodynamic and heat transfer in a geothermal heat exchanger to obtain the optimal diameter of tubes with the lowest entropy using water and Al2O3/water nanofluid. *Geothermics* , *107* (October 2022), 102605. https://doi.org/10.1016/j.geothermics.2022.102605

Klazly, M., & Bognár, G. (2022). A novel empirical equation for the effective viscosity of nanofluids based on theoretical and empirical results. *International Communications in Heat and Mass Transfer* , *135* (April). https://doi.org/10.1016/j.icheatmasstransfer.2022.106054

Kurnia, JC, Putra, ZA, Muraza, O., Ghoreishi-Madiseh, SA, & Sasmito, AP (2021). Numerical evaluation, process design and techno-economic analysis of geothermal energy extraction from abandoned oil wells in Malaysia. *Renewable Energy* , *175* , 868–879. https://doi.org/10.1016/j.renene.2021.05.031

Leong, KY, Razali, I., Ku Ahmad, KZ, Ong, HC, Ghazali, MJ, & Abdul Rahman, MR (2018). Thermal conductivity of an ethylene glycol/water-based nanofluid with copper-titanium dioxide nanoparticles: An experimental approach. *International Communications in Heat and Mass Transfer* , *90* (November 2017), 23–28. https://doi.org/10.1016/j.icheatmasstransfer.2017.10.005

Maheshwary, PB, Handa, CC, & Nemade, KR (2017). A comprehensive study of effect of concentration, particle size and particle shape on thermal conductivity of titania/water based nanofluid. *Applied Thermal Engineering* , *119* , 79–88. https://doi.org/10.1016/j.applthermaleng.2017.03.054

Mohammed, H.I., Giddings, D., Walker, G.S., & Power, H. (2018). CFD assessment of the effect of nanoparticles on the heat transfer properties of acetone/ZnBr2 solution. *Applied Thermal Engineering* , *128* , 264–273. https://doi.org/10.1016/j.applthermaleng.2017.08.169

Qu, C., Zheng, J., Wu, S., Dai, R., & Zhang, J. (2023). Multi-objective optimization of thermal and hydraulic performance with various concentrations of hybrid Fe3O4/graphene nanofluids in a microchannel heat sink. *Case Studies in Thermal Engineering* , *45* (April). https://doi.org/10.1016/j.csite.2023.102963

Safaei, A., Hossein Nezhad, A., & Rashidi, A. (2020). High temperature nanofluids based on thermonol 66 for improving the heat exchangers power in gas refineries. *Applied Thermal Engineering* , *170* (July 2019). https://doi.org/10.1016/j.applthermaleng.2020.114991

Sajid, M.U., & Ali, H.M. (2018). International Journal of Heat and Mass Transfer Thermal conductivity of hybrid nanofluids : A critical review. *International Journal of Heat and Mass Transfer* , *126* , 211–234. https://doi.org/10.1016/j.ijheatmasstransfer.2018.05.021

Salameh, T., Alkasrawi, M., Olabi, AG, Makky, A. Al, & Abdelkareem, M.A. (2023). Experimental and numerical analysis of heat transfer enhancement inside concentric counter flow tube heat exchanger using different nanofluids. *International Journal of Thermofluids* , *20* (September), 100432. https://doi.org/10.1016/j.ijft.2023.100432

Schiffner, D., Banks, J., Rabbani, A., Lefsrud, L., & Adamowicz, W. (2022). Techno-economic assessment for heating cattle feed water with low-temperature geothermal energy: A case study from central Alberta, Canada. *Renewable Energy* , *198* (June), 1105–1120. https://doi.org/10.1016/j.renene.2022.07.006

Shingare, P. P., Kriplani, V. M., & Shelke, R. S. (2012). *Heat Transfer Enhancement of Al 2 O 3 Nanofluid Dispersed in Ethylene Glycol* . *05* (03), 3–5.

Vetter, C., Wiemer, H. J., & Kuhn, D. (2013). Comparison of sub- and supercritical Organic Rankine Cycles for power generation from low-temperature/low-enthalpy geothermal

wells, considering specific net power output and efficiency. *Applied Thermal Engineering , 51* (1–2), 871–879. https://doi.org/10.1016/j.applthermaleng.2012.10.042

Wang, K., Yuan, B., Ji, G., & Wu, X. (2018). A comprehensive review of geothermal energy extraction and utilization in oilfields. *Journal of Petroleum Science and Engineering , 168* (April), 465–477. https://doi.org/10.1016/j.petrol.2018.05.012

Xie, H., Wang, J., Xi, T., Liu, Y., Ai, F., & Wu, Q. (2002). Thermal conductivity enhancement of suspensions containing nanosized alumina particles. *Journal of Applied Physics , 91* (7), 4568–4572. https://doi.org/10.1063/1.1454184

Younes, H., Mao, M., Sohel Murshed, S.M., Lou, D., Hong, H., & Peterson, G.P. (2022). Nanofluids: Key parameters to enhance thermal conductivity and its applications. *Applied Thermal Engineering , 207* (November 2021). https://doi.org/10.1016/j.applthermaleng.2022.118202